ACS APPLIED MATERIALS & INTERFACES

RESEARCH ARTICLE

www.acsami.org

Surface and Buried Interfacial Structures of Epoxy Resins Used as Underfills Studied by Sum Frequency Generation Vibrational Spectroscopy

Anne V. Vázquez,[‡,†] Brad Holden,[†] Cornelius Kristalyn,[†] Mike Fuller,[§] Brett Wilkerson,[§] and Zhan Chen*[,†]

[†]Department of Chemistry, University of Michigan, Ann Arbor, Michigan 48109, United States

[§]Freescale Semiconductor, Inc., 6501 William Cannon Drive West, Austin, Texas 78735, United States

ABSTRACT: Flip chip technology has greatly improved the performance of semiconductor devices, but relies heavily on the performance of epoxy underfill adhesives. Because epoxy underfills are cured *in situ* in flip chip semiconductor devices, understanding their surface and interfacial structures is critical for understanding their adhesion to various substrates. Here, sum frequency generation (SFG) vibrational spectroscopy was used to study surface and buried interfacial structures of two model epoxy resins used as underfills in flip chip devices, bisphenol A digylcidyl ether (BADGE) and 1,4-butanediol diglycidyl ether (BDDGE). The surface structures of these epoxies were compared before and after cure, and the orientations of their surface functional groups were deduced to understand how surface structural changes during cure may affect adhesion properties. Further, the effect of moisture exposure, a known cause of adhesion failure, on surface structures was studied. It was found that the BADGE surface significantly restructured upon moisture exposure while the BDDGE surface did not, showing that BADGE adhesives may be more prone to moisture-induced delamination. Lastly, although surface structure can give some insight into adhesion, buried interfacial structures more directly correspond to adhesion properties of polymers. SFG was used to study buried interfaces between deuterated polystyrene (*d*-PS) and the epoxies before and after moisture exposure. It was shown that moisture exposure acted to disorder the buried interfaces, most likely due to swelling. These results correlated with lap shear adhesion testing showing a decrease in adhesion strength after moisture exposure. The presented work showed that surface and interfacial structures can be correlated to adhesive strength and may be helpful in understanding and designing optimized epoxy underfill adhesives.

KEYWORDS: SFG spectroscopy, surfaces and interfaces, adhesion, epoxy underfills, molecular structures, moisture exposure

1. INTRODUCTION

Applications of flip-chip technology have greatly advanced the semiconductor industry in recent years. However, flip-chip devices require the use of an electronically insulating underfill adhesive, which is generally made of epoxy resin. Bisphenol-type epoxies are the most common material used as underfills, and additives such as aliphatic epoxies, SiO_2 and TiO_2 particle fillers, and silane adhesion promoters are often also included in formulations.[1−6] The epoxies used in underfills are generally cured with primary amines, forming hydroxyl groups in the cured network that can participate in hydrogen bonding.[7]

The success of flip-chip devices largely depends on the underfill adhesive. The underfill adhesive comes into contact with a variety of substrates in semiconductor devices, including metals, semiconductors and polymeric passivation layers. If the adhesion of the underfill adhesive fails at any of these interfaces, the flip-chip device can fail.[3,4,8−11] Thus, it is extremely important to understand the adhesion of epoxies used as underfills.

The adhesion of epoxy underfills can fail for a variety of reasons. One major cause is interfacial stress due to a mismatch of coefficients of thermal expansion between the substrate and adhesive. Because epoxies contact a variety of different adherends in flip-chip devices, this can be a significant problem.[8−11] Another major cause of adhesion failure of underfill epoxy adhesives is moisture exposure, which causes swelling and deformation.[3,4,10,12]

Sum frequency generation (SFG) vibrational spectroscopy has been developed into an analytical technique to study surfaces and buried interfaces. As a nonlinear optical technique, SFG can probe both surfaces and interfaces that are accessible to light.[13−17] SFG allows one to detect the presence, coverage, chemical environment, orientation, and orientational ordering of surface or interfacial species. SFG has been extensively used to characterize polymer surfaces and interfaces including polymer surface structures in air and in water, surface structures of polymer blends and copolymers, polymer−liquid interfaces, solid−polymer interfaces, and polymer−biomolecule interfaces.[18−41]

Because adhesion mechanisms largely depend on interfacial structures and interactions, SFG is an ideal technique to study the buried interfaces between epoxy underfill adhesives and substrates in flip-chip devices. Further, SFG can be used to examine the effect of moisture on surface and interfacial structures to monitor for evidence of water-induced interfacial structural changes.

In this study, SFG was used to investigate model compounds for epoxy resins used as underfills in flip-chip devices. First, surfaces of model bisphenol-type and aliphatic-type epoxy resins were studied. Uncured and cured samples were investigated on two different substrates to determine how substrate affects the deposition of epoxy underfills. As discussed above, underfill materials contact many different types of materials in flip-chip

Received: February 12, 2011
Accepted: April 4, 2011
Published: April 19, 2011

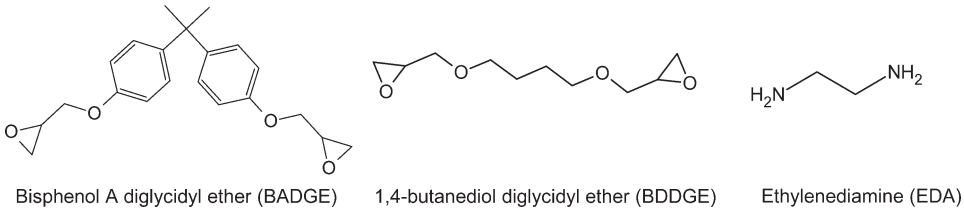

Figure 1. Structures of compounds used in the study.

devices, and if the underfill material deposits differently on different substrates, adhesion could be affected. By comparing surface structures of uncured and cured epoxies, any changes during the cure process that may impact adhesion can be elucidated.

The effect of moisture exposure on cured epoxy surfaces was also investigated with SFG. As described previously, moisture exposure leads to delamination of epoxies. Any moisture-induced delamination mechanism could distort the epoxy surface structure, altering the ability of the epoxy to participate in adhesion mechanisms. Understanding how moisture exposure changes epoxy surface structure may provide further information about how moisture diminishes epoxy adhesion. Lastly, buried interfaces between deuterated polystyrene (*d*-PS) and cured model epoxies were investigated. The *d*-PS was chosen as a model polymer surface because it was fully deuterated, avoiding any spectral confusion with the epoxies. The effect of moisture exposure on buried interfacial structures was investigated. Lap shear adhesion testing was performed on analogous samples to connect adhesion strength to buried interfacial structure.

2. EXPERIMENTAL SECTION

2.1. Materials. Bisphenol A digylcidyl ether (BADGE), 1,4-butanediol diglycidyl ether (BDDGE), ethylene diamine (EDA) and polystyrene (PS, M_V = 280 000) were purchased from Sigma-Aldrich, Inc. Deuterated polystyrene (*d*-PS, M_V = 207 500) was obtained from Polymer Source, Inc. Deuterated polystyrene was used in SFG studies to avoid spectral confusion in the C−H stretching region. All chemicals were used as received.

2.2. Sample Preparation. Thin films of uncured BADGE and BDDGE on fused silica substrates for both SFG and contact angle goniometry analysis were prepared by diluting BADGE or BDDGE to 2 wt % solutions in chloroform (Sigma-Aldrich, Inc.). The diluted solutions were spin-cast on fused silica windows (1-in diameter, 1/8-in thickness, ESCO Products, Inc.) using a spin coater from Specialty Coating Systems. The fused silica windows were cleaned by etching in warm chromic acid solution prior to use. Thin films of uncured BADGE and BDDGE on *d*-PS substrates for SFG and contact angle goniometry analysis were prepared by first spin coating a 1 wt % *d*-PS solution in toluene (Sigma-Aldrich, Inc.) onto fused silica windows that had been cleaned by etching in warm chromic acid. The *d*-PS films were dried in an oven for approximately 18 h at 120 °C and were cooled to room temperature. Then, the 2 wt % solutions of BADGE or BDDGE in chloroform were spin-cast on top of the *d*-PS film.

Thin films of cured BADGE and BDDGE were prepared for SFG analysis by first mixing the BADGE or BDDGE and EDA curing agent in a 2:1 molar ratio. The epoxy and curing agents were diluted to 2 wt % solutions in chloroform. The dilute solutions were spin-cast on fused silica windows that had been etched in warm chromic acid solution. The samples were then cured in an oven for approximately 18 h at 80 °C and were cooled to room temperature prior to analysis. For cured BADGE and BDDGE samples that were exposed to moisture, the cured samples were placed in deionized water for 18 h and dried prior to SFG analysis.

Buried interfaces of *d*-PS and cured BADGE or BDDGE for SFG analysis were prepared as follows. Thin films of *d*-PS were prepared by spin coating the 1 wt % solution of *d*-PS in toluene onto fused silica windows that had been etched in chromic acid prior to sample preparation. The *d*-PS films were dried in an oven at 120 °C for approximately 18 h and were allowed to cool. Then, BADGE or BDDGE were mixed with the EDA curing agent in a 2:1 molar ratio. Thick layers of the undiluted BADGE and EDA or BDDGE and EDA mixtures were deposited onto the *d*-PS thin films. These buried interface samples were cured in an oven at 80 °C for approximately 18 h and were cooled to room temperature prior to SFG analysis. When exposed to moisture, the buried interface samples were placed in deionized water for 18 h and were dried prior to SFG analysis.

Adhesion lap shear samples were prepared as follows. Glass microscope slides (Fisher Scientific, Inc.) were cleaned by etching in warm chromic acid solution. A thin film of PS was deposited on half the glass slides by spin coating a 1 wt % PS solution in toluene on the slides. The slides were dried in an oven at 120 °C for approximately 18 h and were allowed to cool to room temperature. Cured BADGE and BDDGE were prepared by mixing BADGE and BDDGE with the EDA curing agent in a 2:1 molar ratio. Thick films of the BADGE/EDA or BDDGE/EDA mixtures were applied to the *d*-PS films and a second glass slide was placed on top of the BADGE/EDA or BDDGE/EDA thick film such that there was a 1/2 cm bond length. The samples were cured in an oven at 80 °C for approximately 18 h and were cooled to ambient temperature prior to analysis. In lap shear testing, adhesion failure only occurred at the PS/epoxy interface, not the glass/epoxy interface.

Structures of BADGE, BDDGE, and EDA are displayed in Figure 1.

3.3. SFG Experiments. The theory of SFG is well-developed and has been detailed in the literature.[13−17] Further, the experimental setup used in these experiments has alaso been described in previous publications.[18,20,22−24] Briefly, the visible and infrared (IR) input beams overlap spatially and temporally on the polymer surface, polymer/liquid interface or the polymer/cured epoxy interface with input angles of 60 and 54°, respectively, and pulse energies of 200 and 100 μJ, respectively. The beam diameters are approximately 500 μm. Prior results indicate that SFG signals are dominated by polymer surface or interface with negligible contribution from the polymer bulk or the polymer/substrate interface. In this investigation, SFG spectra were obtained in the ssp (s-polarized sum frequency output, s-polarized visible input and p-polarized IR input), ppp, and sps polarization combinations.

3.4. SFG Orientation Analysis. SFG signal in the ssp polarization combination can be used to probe $\chi^{(2)}_{yyz}$, and $\chi^{(2)}_{yyz}$ can be written as the following:

$$\chi^{(2)}_{yyz} = \chi^{(2)}_{R,yyz} + \chi^{(2)}_{NR,yyz} = \sum_q \frac{A_{q,yyz}}{\omega_{IR} - \omega_q + i\Gamma_q} + \chi^{(2)}_{NR,yyz} \qquad (1)$$

where $\chi^{(2)}_{R,yyz}$ is the resonant second-order nonlinear susceptibility component, $\chi^{(2)}_{NR,yyz}$ is the nonresonant second order nonlinear susceptibility component, and A_q, ω_{IR}, ω_q, and Γ_q are the strength of vibrational

mode q, the infrared frequency, the frequency of vibrational mode q, and the damping constant of vibrational mode q, respectively.

The orientation of surface and/or interfacial functional groups can be deduced by fitting SFG spectra obtained using different polarization combinations of the input and output beams because of the relationship between the second-order nonlinear susceptibility, $\chi^{(2)}$, and the second-order nonlinear polarizability, or hyperpolarizability, $\beta^{(2)}$ (we will use β below in this article).

The methyl groups of BADGE can be considered part of an isopropyl group. Here, a procedure first performed by Kataoka and Cremer[42] was used in which the entire $(CH_3)_2C$ unit was treated as a single entity rather than two separate methyl groups. The two methyl groups were considered to have a fixed angle between them of $2\alpha = 112°$, and it was assumed that the two methyl groups could rotate freely, leaving the $(CH_3)_2C$ group with quasi-C_{2v} symmetry. As such, some nonvanishing components of the second-order nonlinear susceptibility, $\chi^{(2)}$ are

$$\chi_{yyz,sym} = N(\beta_{aac} - \beta_{ccc})\{(\cos\alpha - \cos^3\alpha) \times(5 + 3\cos 2\psi) - 2\cos\alpha\}(\cos\theta - \cos^3\theta) - 2(\cos\alpha - \cos^3\alpha)\cos\theta + 2N\beta_{aac}\cos\alpha\cos\theta \quad (2)$$

$$\chi_{yzy,sym} = N(\beta_{aac} - \beta_{ccc})\{(\cos\alpha - \cos^3\alpha) \times(5 + 3\cos 2\psi)(\cos\theta - \cos^3\theta) + 2\cos\alpha\cos\theta(\cos^2\alpha + \cos^2\theta - 2)\} \quad (3)$$

$$\chi_{zzz,sym} = N(\beta_{aac} - \beta_{ccc})(\cos\alpha - \cos^2\alpha)[\{2\cos^3\theta - 3(1 + \cos 2\psi)(\cos\theta - \cos^3\theta)\} - 2\cos\alpha\cos^3\theta] + 2N\beta_{aac}\cos\alpha\cos\theta \quad (4)$$

$$\chi_{yyz,asym} = N\beta_{caa}[(\cos\alpha - \cos^3\alpha)\{-2\cos\theta + 3(\cos\theta - \cos^3\theta)(1 + \cos 2\psi)\} - 2\cos^3\alpha(\cos\theta - \cos^3\theta)] \quad (5)$$

$$\chi_{yzy,asym} = N\beta_{caa}[3(\cos\alpha - \cos^3\alpha) \times (\cos\theta - \cos^3\theta)(1 + \cos 2\psi) + 2\cos^3\alpha\cos^3\theta] \quad (6)$$

$$\chi_{zzz,asym} = 2N\beta_{caa}[(\cos\alpha - \cos^3\alpha)\{2\cos\theta - 3(\cos\theta - \cos^3\theta)(1 + \cos 2\psi)\} + 2\cos^3\alpha(\cos\theta - \cos^3\theta)] \quad (7)$$

where β_{aac}, β_{caa}, and β_{ccc} are elements of the hyperpolarizability tensor and N is the number density of the detected molecules. The angle α is a constant of 56°. By detecting and fitting SFG signal in different polarization combinations, ratios of the $\chi^{(2)}$ elements can be calculated and used to determine values of the tilt and twist angles, θ and ψ, respectively. In the above equations, we assumed that both $\theta$and ψ have δ-angle distributions. Also in this study, the twist angle,ψ, was assumed to have free rotation and thus was averaged. For these studies, the value of β_{aac}/β_{aac} used was 3.4 and the ratio of $\chi_{yyz,sym}/\chi_{yzy,asym}$ for the methyl groups was used.[42]

To calculate the orientation of BDDGE methylene groups, we performed a similar analysis for methylene groups. The nonvanishing components of the second-order nonlinear susceptibility can be written as the following:[24,43−45]

$$\chi_{yyz,sym} = \frac{1}{4}N(\beta_{aac} + \beta_{bbc} + 2\beta_{ccc}) + 2\beta_{ccc}\cos\theta + \frac{1}{4}N(\beta_{aac} + \beta_{bbc} - 2\beta_{ccc})\cos^3\theta \quad (8)$$

$$\chi_{yzy,sym} = \frac{-1}{4}N(\beta_{aac} + \beta_{bbc} - 2\beta_{ccc})(\cos\theta - \cos^3\theta) \approx 0 \quad (9)$$

$$\chi_{zzz,sym} = \frac{1}{2}N(\beta_{aac} + \beta_{bbc})\cos\theta - \frac{1}{2}N(\beta_{aac} + \beta_{bbc} - 2\beta_{ccc})\cos^3\theta \quad (10)$$

$$\chi_{yyz,asym} = \frac{-1}{2}N\beta_{caa}(\cos\theta - \cos^3\theta) \quad (11)$$

$$\chi_{yzy,asym} = \frac{-1}{2}N\beta_{caa}\cos^3\theta \quad (12)$$

$$\chi_{zzz,asym} = N\beta_{caa}(\cos\theta - \cos^3\theta) \quad (13)$$

where β_{aac}, β_{bbc}, β_{ccc}, and β_{caa} are elements of the hyperpolarizability tensor and N is the number density of the detected molecules. In the current study, as the study above of BADGE methyl groups, a δ-distribution of methylene groups was assumed.

Like the methyl group orientation analysis described above, the orientation of methylene groups can be determined by fitting SFG spectra obtained using different polarization combinations of the input and output beams to determine elements of the second-order nonlinear susceptibility. Ratios of the $\chi^{(2)}$ elements can then be used to determine orientation angle, θ. Here, the ratio $\chi_{yyz,sym}/\chi_{yzy,asym}$ was used with a β_{ccc}/β_{aac} value of 0.14.[45]

The orientation of the phenyl groups of BADGE can also be determined using similar analysis. The phenyl groups of BADGE are para-substituted, and therefore can be thought to have local C_{2v} symmetry. If it is assumed that the BADGE surface is azimuthally isotropic, two angles must be considered: the tilt angle (θ) and the twist angle (ψ). Like the methyl group analysis, we assumed that the twist angle ψ has free rotation and therefore was averaged.

The components of the second order nonlinear susceptibility, $\chi^{(2)}$ can be written as the following for the A1 and B1 irreducible representations[46−49]

$$\chi_{yyz,A1} = \frac{N_s}{8}[\beta_{aac,A1}\cos\theta(3 + \cos 2\theta - 2\sin^2\theta\cos 2\psi) + \beta_{bbc,A1}\cos\theta(3 + \cos 2\theta + 2\sin^2\theta\cos 2\psi) + \beta_{ccc,A1}(\cos\theta - \cos 3\theta)] \quad (14)$$

$$\chi_{yzy,A1} = \frac{N_s}{16}[-\beta_{aac,A1}(\cos\theta - \cos 3\theta)(1 + \cos 2\psi) - \beta_{bbc,A1}(\cos\theta - \cos 3\theta)(1 - \cos 2\psi) + 2\beta_{ccc,A1}(\cos\theta - \cos 3\theta)] \quad (15)$$

$$\chi_{yyz,B1} = -\frac{N_s}{8}\beta_{aca,B1}(\cos\theta - \cos 3\theta)(1 + \cos 2\psi) \quad (16)$$

$$\chi_{yzy,B1} = \frac{N_s}{8}\beta_{aca,B1}[4\cos\theta - (\cos\theta - \cos 3\theta)(1 + \cos 2\psi)] \quad (17)$$

The A1 irreducible representation consists of the ν_2 and ν_{20a} phenyl modes while the B1 irreducible representation consists of the ν_{7b} and the ν_{20b} phenyl modes. Using the bond additivity approach, ratios of the nonzero β terms can be determined to be the following for para-substituted phenyl rings:[43,44,49,50]

$$\frac{\beta_{ccc,\nu2}}{\beta_{aac,\nu2}} = 0.69,\ \frac{\beta_{bbc,\nu2}}{\beta_{aac,\nu2}} = 0.04,\ \frac{\beta_{aca,\nu7b}}{\beta_{aac,\nu2}} = 0.47$$

The only mode observed in SFG spectra of BADGE was the ν_2 mode at 3060 cm^{-1}. For this mode, the appropriate χ ratio was calculated to be

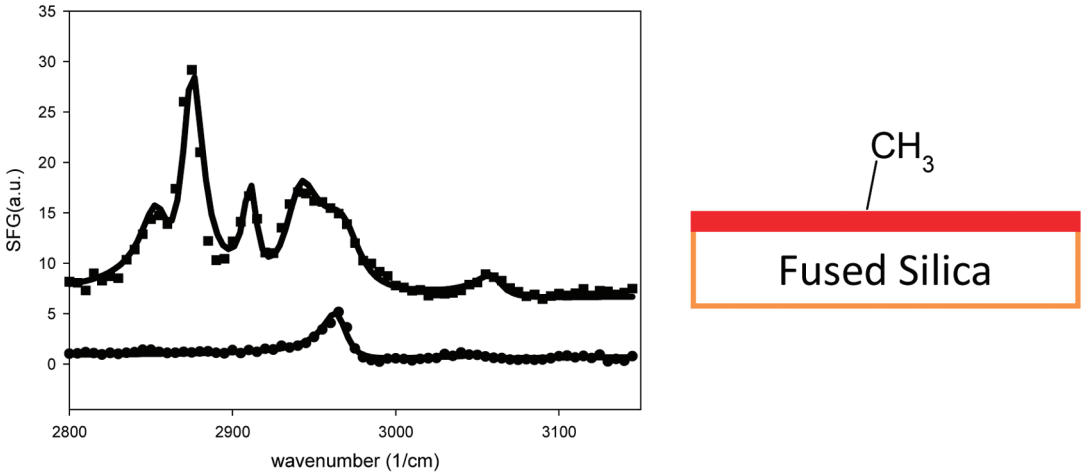

Figure 2. Left: SFG spectra of uncured BADGE on fused silica in ssp (squares) and sps (circles). Solid lines are spectral fits. Right: Schematic showing that BADGE surface methyl groups tilt at 15° vs the surface normal.

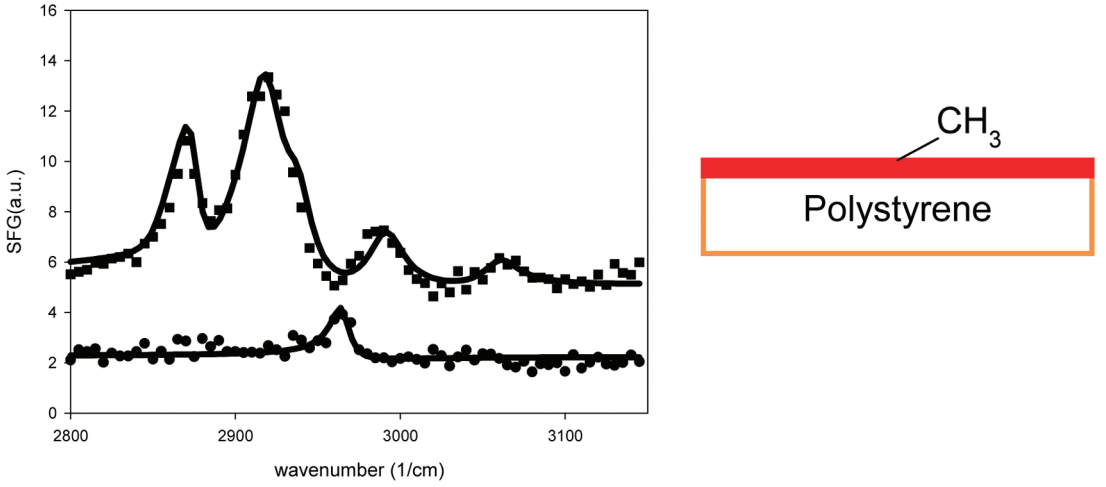

Figure 3. Left: SFG spectra of uncured BADGE on *d*-PS in ssp (squares) and sps (circles). Solid lines are spectral fits. Right: Schematic showing that BADGE surface methyl groups tilt at 69° vs the surface normal.

the following:

$$\frac{\chi_{yyz,\nu 2}}{\chi_{yzy,\nu 2}} = \frac{25.4\cos\theta - \cos 3\theta - 11.3\cos\theta\sin^2\theta\cos 2\phi}{(\cos\theta - \cos 3\theta)(1 - 2.82\cos 2\phi)} \quad (18)$$

3.5. Contact Angle Goniometry Experiments. Static water contact angle goniometry measurements were performed using a CAM 100 Optical Contact Meter (KSV Instruments) contact angle goniometer. Samples of uncured BADGE and uncured BDDGE on fused silica and *d*-PS substrates were studied. Eight measurements were performed for each sample.

3.6. Lap Shear Adhesion Testing Experiments. Lap shear adhesion tests were performed using an Instron 5544 Mechanical Testing System. Lap shear tests were performed using ASTM International Standard D3163_01 on cured BADGE before and after moisture exposure and cured BDDGE before moisture exposure. Ten samples of BADGE and BDDGE were tested for each set of adhesion tests.

3. RESULTS AND DISCUSSION

3.1. SFG and Contact Angle Goniometry Studies of Uncured BADGE and BDDGE on Fused Silica and d-PS Substrates. As discussed in the Introduction, epoxies used as underfills in flip-chip devices are deposited into the devices prior to cure, and come into contact with a variety of substrates in the devices. If the epoxies used as underfills deposit differently on different substrates, their surface structures may be altered, affecting how the epoxies adhere to other materials in flip-chip devices. In this study, thin films of uncured BADGE and BDDGE were deposited on fused silica and *d*-PS substrates. As stated in the Introduction, *d*-PS was used as a model polymer for polymeric passivation layers used in flip-chip devices.

Figures 2 and 3 show fitted SFG spectra of uncured BADGE on fused silica and *d*-PS, respectively. Further, Tables 1 and 2 show the fitting parameters used. The peak assignments in the C−H stretching frequency region have been widely reported.[16,36,46,51−53] The SFG ssp spectrum of uncured BADGE on fused silica was dominated by symmetric and asymmetric methyl stretches at 2875 and 2970 cm^{-1}, respectively. There were also symmetric and asymmetric methylene stretches at 2855 and 2912 cm^{-1}, respectively, a Fermi resonance (FR) at 2940 cm^{-1}, and phenyl C−H stretching at 3060 cm^{-1}.

Table 1. Fitting Parameters for ssp Spectrum of Uncured BADGE on Fused Silica

	ssp						sps	
frequency	2855	2875	2912	2940	2970	3060	2965	3055
strength	19.0	33.8	−20.2	46.0	−45.0	13.6	17.2	4.27
width	10.2	7.86	5.05	12.0	14.4	9.6	8.65	9.76
assignment	CH_2 sym	CH_3 sym	CH_2 asym	FR	CH_3 asym	phenyl	CH_3 as	phenyl

Table 2. Fitting Parameters Used for ssp and sps Spectrum of Uncured BADGE on *d*-PS

	ssp						sps
frequency	2855	2875	2920	2938	2994	3060	2965
strength	−8.00	11.7	32.9	13.0	16.5	11.5	9.49
width	15.0	8.33	14.7	11.5	13.2	13.1	7.00
assignment	CH_2 sym	CH_3 sym	CH_2 asym	FR	epoxy sym	phenyl	CH_3 as

For both cases, the sps spectra were dominated by the asymmetric methyl stretch at 2965 cm^{-1} and weak phenyl signal at 3055 cm^{-1}. On *d*-PS, the uncured BADGE signal was dominated by symmetric methyl signal at 2875 cm^{-1}. Other peaks were the symmetric and asymmetric methylene stretches at 2855 and 2920 cm^{-1}, respectively, a Fermi Resonance at 2938 cm^{-1} and a phenyl stretch at 3060 cm^{-1}. Also interestingly, signal at 2995 cm^{-1} was observed when the uncured BADGE was deposited on *d*-PS, and attributed to the symmetric stretch of the epoxy ring.[54] The surface epoxy rings stood up when BADGE was deposited on *d*-PS. However, epoxy rings were either not present on the surface or laid down on the surface when BADGE was deposited on fused silica.

The spectra were fit according to eq 1 and the ratio of $\chi_{yyz,sym}/\chi_{yzy,asym}$ was calculated for surface methyl groups of uncured BADGE on fused silica and *d*-PS. Orientation analysis of the surface methyl groups was performed according to the procedure described previously. Assuming a δ-distribution of angles, it was found that on fused silica, the surface methyl groups of uncured BADGE exhibited a 15° angle with respect to the surface normal while on *d*-PS, the surface methyl groups of uncured BADGE exhibited a 69° angle with respect to the surface normal. Therefore, the orientation of the uncured BADGE methyl groups changed significantly with substrate. On the hydrophilic fused silica surface, the methyl groups stood up, whereas on the hydrophobic *d*-PS surface, the methyl groups laid down more. Further, the epoxy groups stood up on the *d*-PS surface, whereas they did not on the fused silica surface.

The ssp SFG spectra of uncured BDDGE on fused silica and of uncured BDDGE on *d*-PS are shown in Figures 4 and 5, respectively. Also, Tables 3 and 4 show the spectral fitting parameters. When deposited on fused silica, the uncured BDDGE surface ssp spectrum was dominated by peaks at 2855 and 2915 cm^{-1}, corresponding to the symmetric and asymmetric methylene stretches, respectively. Further, an unassigned peak was observed at 2830 cm^{-1}, a Fermi Resonance was observed at 2935 cm^{-1}, and the symmetric epoxy stretch was observed at 3000 cm^{-1}. This indicated that in addition to the methylene groups, the epoxy groups were also present and ordered at the surface. When deposited on *d*-PS, the ssp spectrum of BDDGE was very similar. The spectrum was dominated by the symmetric and asymmetric methylene stretches at 2855 and 2915 cm^{-1}, respectively. There was also the unassigned signal at 2830 cm^{-1}, Fermi resonance signal at 2935 cm^{-1}, and symmetric epoxy stretching at 3000 cm^{-1}. Therefore, from observing the SFG spectra, it appeared that the BDDGE surface was largely unaffected by substrate.

The orientation of the surface uncured BDDGE methylene groups on fused silica and *d*-PS was deduced using the fitting parameters and procedure detailed earlier, using the ratio of $\chi_{yyz,sym}/\chi_{yzy,asym}$. On fused silica, assuming a δ-distribution of methylene orientation angles, the surface BDDGE methylene groups was found to have an orientation angle of 29° with respect to the surface normal. Likewise, on *d*-PS, the surface uncured BDDGE methylene groups were also determined to have an orientation angle of 29° with respect to the surface normal. That is, the orientation of the uncured BDDGE surface methylene groups was unaffected by substrate.

The BADGE surface structures were significantly altered by deposition on the two different substrates, while the BDDGE surface structures were largely unaffected by substrate. Specifically, the BADGE methyl orientation and the BADGE epoxy orientation were different on the different substrates. The BDDGE surface methylene orientation was largely unchanged by substrate, and the epoxy groups were present at the BDDGE surface on both substrates. Perhaps specific interactions between the aromatic rings in BADGE and the surface aromatic groups of *d*-PS caused the BADGE to orient differently when deposited on that substrate, while such interactions did not occur between BDDGE and *d*-PS because there were no aromatic groups in BDDGE to interact with the *d*-PS.

The static water contact angle goniometry measurements for uncured BADGE and BDDGE on fused silica and *d*-PS substrates are reported in Table 5. The BADGE water contact angle was different on the fused silica and *d*-PS substrates. This agreed with SFG results showing that interactions between BADGE and *d*-PS may have caused the BADGE to deposit differently on that substrate. Conversely, the water contact angle for BDDGE was not significantly different on the fused silica and *d*-PS substrates, showing that the surface was not significantly altered by substrate.

To summarize, SFG and contact angle goniometry studies of uncured BADGE and BDDGE on fused silica and *d*-PS substrates showed that the bisphenol-type epoxy deposited differently on the fused silica and *d*-PS substrates. The BDDGE surface structures were not significantly affected by substrate. BADGE molecules contain aromatic groups, which may interact with PS surface phenyl groups more favorably compared to the fused silica surface; therefore BADGE exhibited different surface structures deposited on *d*-PS and fused silica. Specifically, the BADGE surface methyl orientation was affected by substrate. Also, the BADGE epoxy groups stood up when deposited on *d*-PS, while these groups either laid down or were not present on the surface when BADGE was deposited on fused silica.

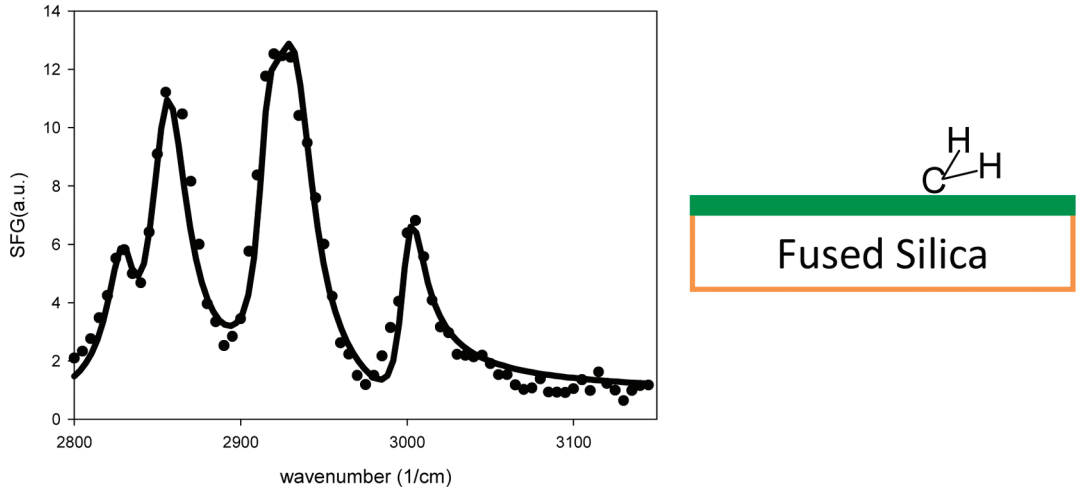

Figure 4. Left: SFG spectrum of uncured BDDGE on fused silica in ssp (circles). Solid line is spectral fit. Right: Schematic showing that BDDGE surface methylene groups tilt at 29° vs the surface normal.

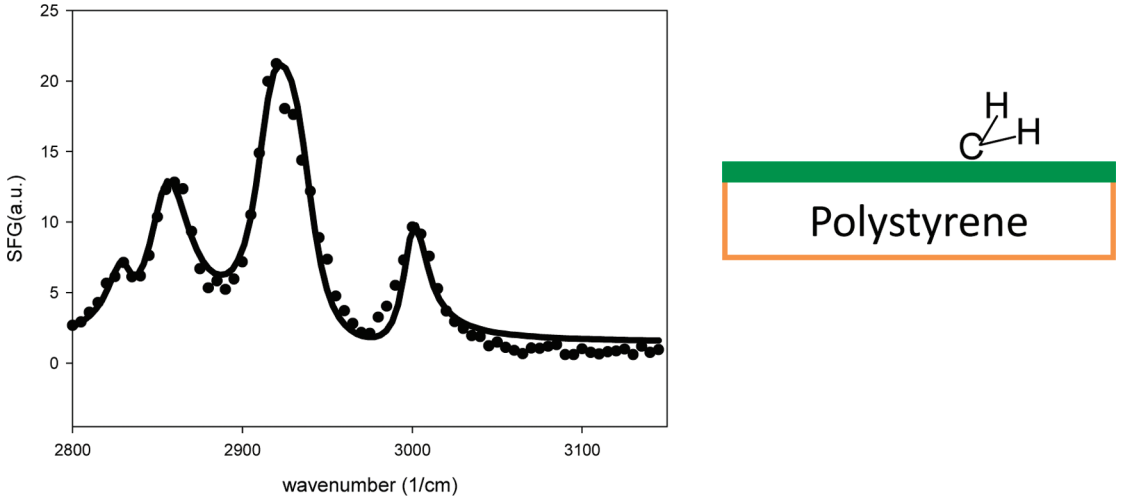

Figure 5. Left: SFG spectrum of uncured BDDGE on *d*-PS in ssp (circles). Solid line is spectral fit. Right: Schematic showing that BDDGE surface methylene groups tilt at 29° vs the surface normal.

Table 3. Fitting Parameters Used for ssp Spectrum of Uncured BDDGE on Fused Silica

frequency	2830	2855	2915	2935	3000
strength	13.8	40.6	−39.1	60.7	15.5
width	10.0	13.4	7.92	15.0	8.44
assignment		CH_2 sym	CH_2 asym	FR	epoxy sym

Table 4. Fitting Parameters Used for ssp Spectrum of Uncured BDDGE on *d*-PS

frequency	2830	2855	2915	2935	3000
strength	10.2	49.2	−76.5	71.2	22.5
width	8.65	15.0	13.3	15.0	8.54
assignment		CH_2 sym	CH_2 asym	FR	epoxy sym

Conversely, BDDGE molecules do not contain aromatic groups and therefore may have similar interactions with *d*-PS and fused silica, so the surface structures were largely unaffected by

Table 5. Static Water Contact Angle Goniometry Results for Uncured BADGE and BDDGE Deposited on Fused Silica and *d*-PS Substrates

	BADGE angle (deg)	BDDGE angle (deg)
water contact angle with fused silica substrate	47.8 ± 11.5	30.3 ± 1.5
water contact angle with *d*-PS substrate	79.0 ± 5.6	21.3 ± 7.7

substrate. Often, specific epoxy underfill surface structures are required for adhesion mechanisms to occur, and if the epoxy surface structures are changed because of the substrate, adhesion can be diminished. Therefore, the effect of the various substrates encountered by underfills in flip-chip devices needs to be considered when designing underfill materials.

3.2. SFG Studies of Cured Epoxy Surfaces and the Effect of Moisture Exposure on Cured Epoxy Surface Structures. Epoxies used as underfills are cured *in situ* in the flip-chip device. Thus, any surface structural changes that occur during the cure process can impact the adhesion of underfills to the various

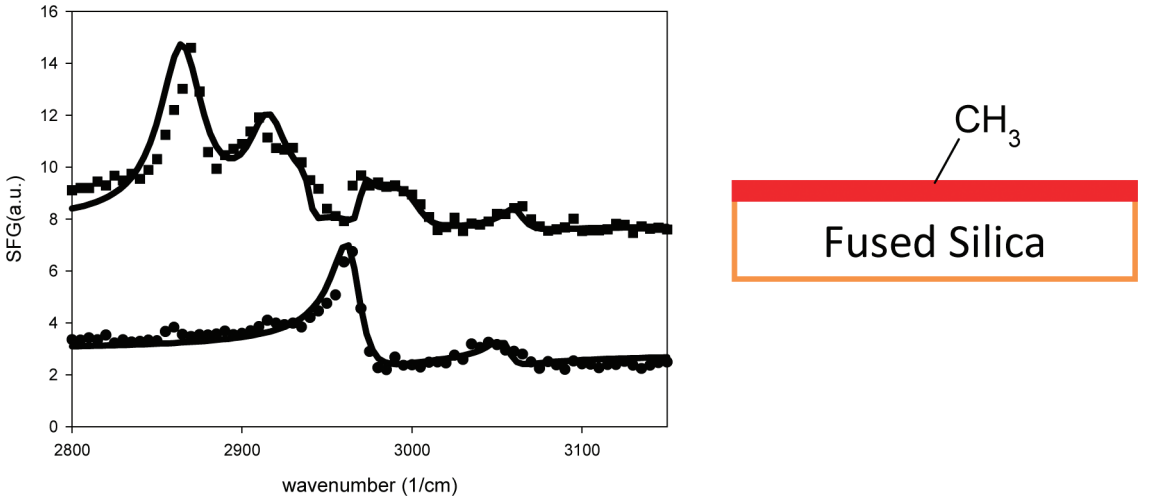

Figure 6. Left: SFG spectra of cured BADGE in ssp (squares) and sps (circles). Solid lines are spectral fits. Right: Schematic showing that BADGE surface methyl groups tilt at 31° vs the surface normal.

Table 6. Fitting Parameters Used for ssp and sps Spectrum of Cured BADGE

	ssp							sps	
frequency	2855	2870	2915	2940	2970	3000	3062	2965	3055
strength	1.78	41.5	−34.6	3.11	−3.27	11.9	5.78	18.8	4.86
width	15.0	15.0	14.5	4.52	4.24	13.7	7.64	10.0	6.66
assignment	CH_2 sym	CH_3 sym	CH_2 asym	FR	CH_3 asym	epoxy sym	phenyl	CH_3 as	phenyl

substrates in flip-chip devices. For example, if the surface structure of an uncured epoxy allows a specific adhesion mechanism to occur, any change in that surface structure after the cure process would diminish the ability of the epoxy to participate in that mechanism. Here, SFG was used to probe the surface structures of BADGE and BDDGE surfaces after they were cured with EDA. Further, the effect of moisture exposure on the surface structures of the two epoxies was investigated. Moisture exposure is known to cause delamination of epoxies. Studying how surface structures of cured epoxies are affected by moisture exposure can help further explain how moisture exposure affects epoxy adhesion.

Figure 6 shows SFG spectra of BADGE after it was cured. Table 6 show the fitting parameters used for the ssp and sps SFG spectra. From observing the spectra, it is apparent they were different than those of the uncured BADGE. The ssp spectrum has peaks at 2855 cm^{-1} and 2915 cm^{-1}, corresponding to the symmetric and asymmetric methylene stretches, respectively. Further, there are peaks at 2870 and 2970 cm^{-1} from the symmetric and asymmetric methyl stretches. There is also Fermi resonance signal at 2940 cm^{-1}, phenyl stretching signal at 3062 cm^{-1}, and symmetric epoxy stretching at 3000 cm^{-1}. The signal at 3000 cm^{-1} indicated that the sample was not completely cured. However, the signal at 3000 cm^{-1} was quite weak and indicated that only a very small amount of uncured epoxy remained. In the sps polarization combination, signal was observed at 2965 cm^{-1}, corresponding to the asymmetric methyl stretch and at 3055 cm^{-1}, corresponding to a phenyl stretch.

The SFG spectra were fit according to eq 1, and orientation analysis of the surface methyl groups was performed. The ratio of $\chi_{yyz,sym}/\chi_{yzy,asym}$ was calculated and the angle of the methyl groups with respect to the surface normal was deduced, assuming a δ-distribution of methyl angles. It was calculated that the cured BADGE surface methyl groups were at a 31° angle with respect to the surface normal. Interestingly, this orientation was different than that of the uncured BADGE methyl groups on either fused silica or *d*-PS, indicating that the surface methyl groups reoriented during the cure process.

Figure 7 shows SFG spectra of cured BADGE after moisture exposure, and Table 7 shows the fitting parameters used for the ssp and sps spectra. After moisture exposure, the ssp spectrum contained peaks at 2869 and 2965 cm^{-1}, corresponding to the symmetric and asymmetric methyl stretches, respectively. Further, peaks were observed at 2912 cm^{-1}, from the asymmetric methylene stretch, 2940 cm^{-1} from a Fermi resonance, 3000 cm^{-1} from the epoxy symmetric stretch, and 3060 cm^{-1} from phenyl stretching. Interestingly, after moisture exposure, the phenyl signal was much stronger than it was before moisture exposure. Therefore, moisture exposure caused the phenyl groups to reorient such that they were standing up more. A similar phenomenon was observed using SFG for a phenolic resin. In the phenolic resin study, it was believed that water formed hydrogen bonds with the oxygen atoms near the aromatic rings, dragging the aromatic rings toward the surface normal.[47] This surface restructuring could diminish adhesion if the structure after moisture exposure was not favorable for adhesion mechanisms. The sps spectrum was dominated by signal at 2965 cm^{-1} from the methyl asymmetric stretch and weaker signal at 3055 cm^{-1} from a phenyl stretch.

The spectra were fit according to eq 1, and the ratio of $\chi_{yyz,sym}/\chi_{yzy,asym}$ for the surface methyl groups was calculated after moisture exposure. When orientation analysis was performed,

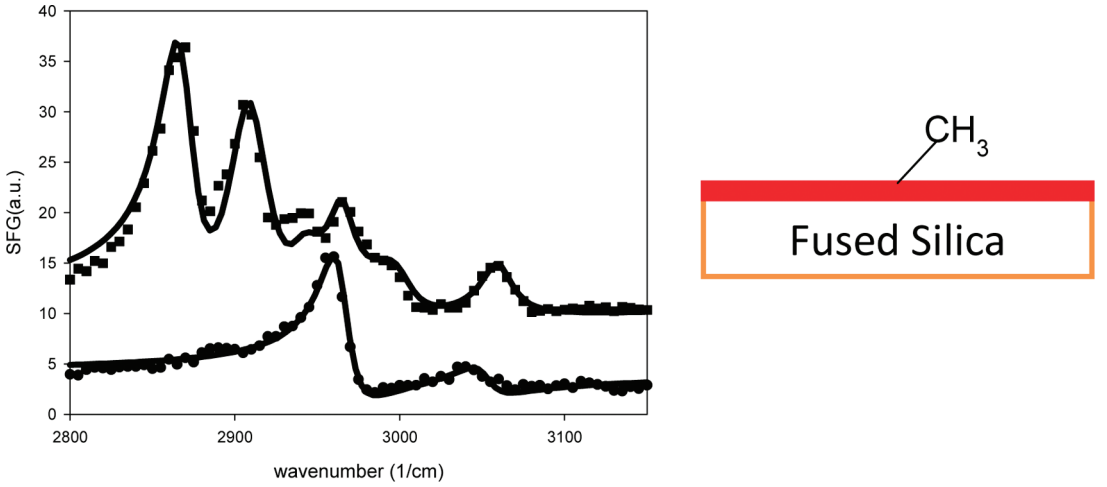

Figure 7. Left: SFG spectra of cured BADGE after moisture exposure in ssp (squares) and sps (circles). Solid lines are spectral fits. Right: Schematic showing that BADGE surface methyl groups tilt at 47° vs the surface normal.

Table 7. Fitting Parameters Used for ssp and sps Spectrum of Cured BADGE after moisture exposure

	ssp					
frequency	2869	2912	2940	2965	3000	3060
strength	46.7	61.8	16.0	−39.3	26.4	24.3
width	12.4	15.0	12.0	9.28	15.0	11.9
assignment	CH_3 sym	CH_2 asym	FR	CH_3 asym	epoxy sym	phenyl

	ssp	
frequency	2965	3055
strength	30.6	10.8
width	10.5	12.0
assignment	CH_3 as	phenyl

assuming a δ-distribution of surface methyl orientation, the surface methyl groups were found to be at a 47° angle with respect to the surface normal. This showed that the surface methyl groups laid down more after being exposed to moisture. This change in surface orientation could affect adhesion properties after moisture exposure. The ratio of $\chi_{yyz,\nu_2}/\chi_{yzy,\nu_2}$ for the phenyl ν_2 stretches were also calculated using the fitting parameters from the cured BADGE and from the cured BADGE after moisture exposure. The ratio for cured BADGE before moisture exposure was 1.04 while the ratio for cured BADGE after moisture exposure was 2.27. We attempted to perform the phenyl orientation analysis. However, the ratios from the experimental results were out of the range of the calculated orientation. This indicates that twist angle is not random and cannot be averaged.[51] The one measurement obtained with SFG is not enough for the accurate determination of the twist angle and tilt angle at the same time, and thus we cannot provide a detailed, quantitative description of the phenyl group orientation here.

The SFG spectrum of cured BDDGE is shown in Figure 8, and its fitting parameters are shown in Table 8. The cured BDDGE ssp spectrum was dominated by symmetric and asymmetric methylene stretching at 2855 and 2915 cm^{-1}. There was also unassigned signal at 2830 cm^{-1} and Fermi resonance signal at 2935 cm^{-1}. Of note, the peak at 3000 cm^{-1} was absent after cure, indicating that the BDDGE surface was largely cured.

Spectral fitting and orientation analysis was performed by calculating the ratio of $\chi_{yyz,sym}/\chi_{yzy,asym}$ for the surface methylene groups and using this ratio to determine the angle of the methylene groups with respect to the surface normal, assuming a δ-distribution. Here, the orientation angle of the methylene groups was calculated to be 28°. This was nearly identical to the methylene orientation calculated for uncured BDDGE, showing that the BDDGE methylene structure did not change significantly after the system was cured.

Lastly, the cured BDDGE thin films were exposed to moisture, and this spectrum and its fit are shown in Figure 9 and the fit parameters are seen in Table 9. After moisture exposure, the cured BDDGE surface was still dominated by symmetric and asymmetric methylene stretches at 2855 and 2915 cm^{-1}, respectively, as well as an unassigned peak at 2830 cm^{-1}.

Spectral fitting and orientation analysis of the BDDGE methylene groups revealed that after moisture exposure, the BDDGE methylene groups exhibited a 28° angle with respect to the surface normal. This orientation angle is nearly the same as the cured and uncured BDDGE. Therefore, BDDGE methylene orientation was largely unaffected by curing and by moisture exposure.

The studies of cured BADGE and BDDGE showed that the surface structures of epoxies can change with cure. The orientation of the BADGE surface methyl groups changed with cure. The spectra of the cured BDDGE surface showed evidence of the curing reaction occurring at the surface, because the epoxy ring signal disappeared. However, the orientation of the BDDGE methylene groups did not change significantly with cure. These studies demonstrated that SFG can be used to monitor surface cure reactions and cure-induced structural changes that may affect the adhesion of underfills in flip-chip devices.

Further, these studies demonstrated the effect of moisture exposure on cured epoxy surfaces. Understanding how moisture affects epoxy surfaces is of great importance because moisture exposure can cause adhesion failure. While the BDDGE surface structure did not significantly change after moisture exposure, the BADGE surface did restructure, in that the methyl orientation changed and the phenyl groups reordered toward the surface

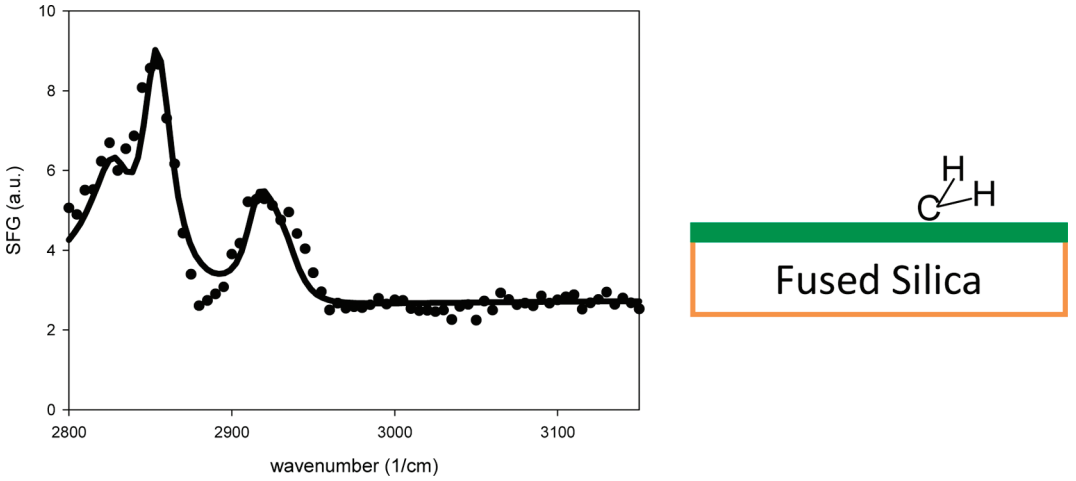

Figure 8. Left: SFG spectrum of cured BDDGE in ssp (circles). Solid line is spectral fit. Right: Schematic showing that BDDGE surface methylene groups tilt at 28° vs the surface normal.

Table 8. Fitting Parameters Used for ssp spectrum of cured BDDGE

frequency	2830	2855	2915	2935
strength	16.92	24.51	−22.93	20.42
width	15	11.04	10.62	15
assignment		CH_2 sym	CH_2 asym	FR

normal. The restructuring of the BADGE surface with moisture exposure could affect how it could participate in adhesion mechanisms and needs to be considered when formulating underfills.

3. SFG and Lap Shear Adhesion Testing Studies of the Buried Interfaces Between d-PS and Cured Epoxies and the Effect of Moisture Exposure on the Buried Interfaces Between d-PS and Cured Epoxies. While the earlier studies were important in developing a fundamental understanding of the surface structures of BADGE and BDDGE, they were not sufficient to understand the adhesion of epoxies used as underfills in flip-chip devices. Interfacial mechanisms between adhesive and adherend largely define adhesion, so the buried interfacial structures between the two materials need to be understood. These buried interfacial structures can be different from the adhesive surface structures due to interactions with the adherend.

Here, studies of the buried interfacial structures between *d*-PS thin films and thick cured BADGE or BDDGE films were investigated with SFG. Before that research, SFG studies were conducted of the buried interfaces between *d*-PS thin films and thick uncured BADGE or BDDGE films. However, no SFG signal was observed for any of these buried interfaces (not shown). It was concluded that the buried interfaces between *d*-PS and uncured BADGE and BDDGE were disordered. That is, the uncured BADGE and BDDGE adopted random interfacial structures.

The effect of moisture on the *d*-PS/cured BADGE and *d*-PS/cured BDDGE interfaces was also investigated. SFG spectra of the buried interfaces were obtained after moisture exposure to determine if and how moisture affects any ordered buried interfacial structures at the *d*-PS/cured epoxy interface. Any moisture-induced changes in buried interfacial structure may help to further explain why moisture causes epoxy underfill delaminanation in flip-chip devices.

Lastly, lap shear adhesion testing was performed on PS/cured epoxy interfaces to determine how moisture exposure affected the adhesion strength between PS and the epoxies. Adhesion strength, as measured by the adhesion strength in MPa for lap-shear adhesion, was correlated to buried interfacial structure of the epoxies.

Figure 10 shows SFG spectra in the ssp polarization combination of the *d*-PS/cured BADGE buried interface before and after moisture exposure. In Figure 10, in the spectrum with closed circles, weak signal between 2910 and 2940 cm^{-1} can be attributed to methylene signal from the *d*-PS/cured BADGE buried interface. Unlike the uncured BADGE, the cured BADGE appeared to have some orientational order at the buried *d*-PS interface. However, the signal decreased after the *d*-PS/cured BADGE buried interface was exposed to moisture , as seen in the spectrum with the open circles. Because of moisture absorption, the buried interface became deformed and the interfacial orientational order of the BADGE was lost. This was most likely due to moisture-induced swelling of the epoxy.

Figure 11 shows ssp SFG spectra of the *d*-PS/cured BDDGE buried interface before and after moisture exposure. Prior to moisture exposure, signal at 2850 cm^{-1} was attributed to the methylene symmetric stretch of the BDDGE at the buried interface. While the uncured BDDGE did not order at the *d*-PS buried interface, after the cure process, the cured BDDGE did exhibit some interfacial ordering, showing interfacial structural changes during the cure process. This interfacial ordering may contribute to adhesion. Further, after the *d*-PS/cured BDDGE buried interface was exposed to moisture, the symmetric methylene signal decreased significantly. Like the *d*-PS/cured BADGE interface, moisture exposure caused the buried interface to become disordered, most likely because swelling deformed the epoxy.

The lap-shear adhesion testing results are shown in Table 10. After cure, both the BADGE and BDDGE showed adhesion to PS, as measured by the adhesion strength in MPa for lap-shear adhesion. The adhesion correlated to more ordered buried interfacial structures. It is possible that the buried interfacial orientational ordering of the epoxies promoted stronger adhesion. After moisture exposure, the adhesion decreased for both epoxies. The BDDGE adhesion strength decreased to negligible amounts while the BADGE adhesion strength decreased significantly

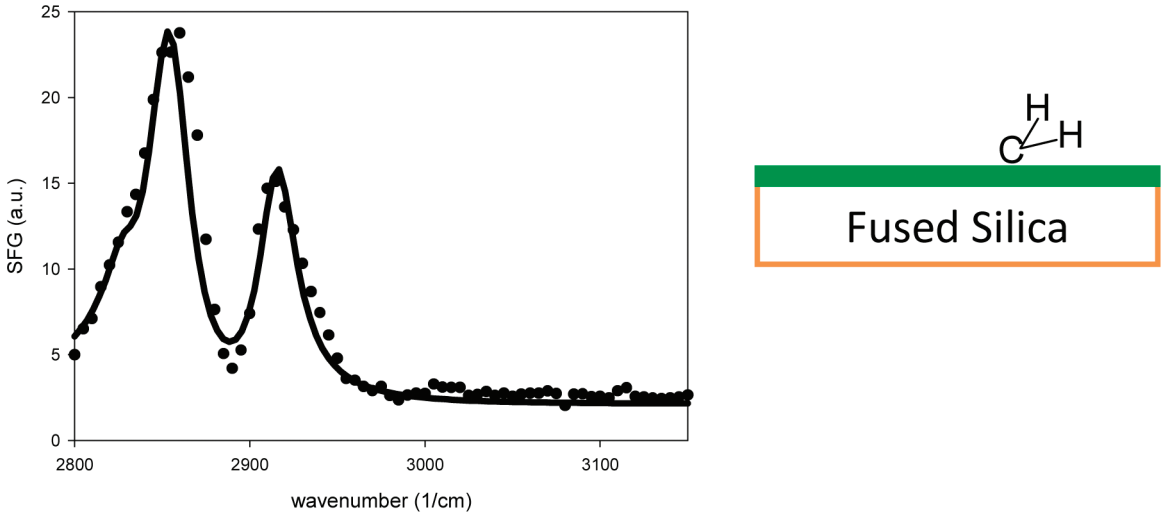

Figure 9. Left: SFG spectrum of cured BDDGE after moisture exposure in ssp (circles). Solid line is spectral fit. Right: Schematic showing that surface methylene groups tilt at 28° vs the surface normal.

Table 9. Fitting Parameters Used for ssp Spectrum of Cured BDDGE after Moisture Exposure

frequency	2830	2855	2915
strength	7.83	73.3	−54.6
width	10.8	15.0	13.0
assignment		CH_2 sym	CH_2 asym

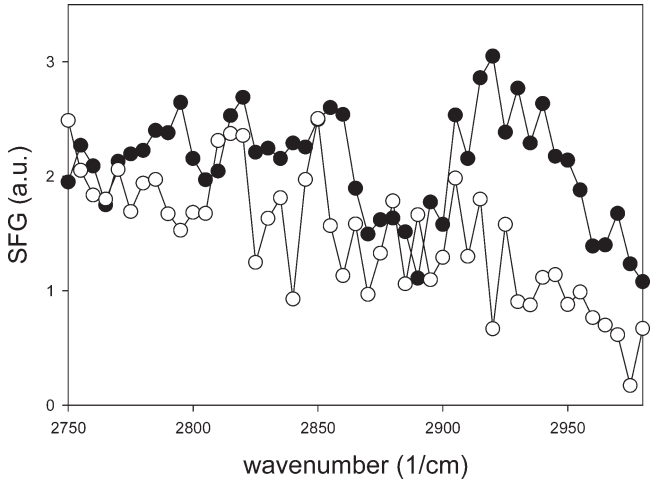

Figure 10. SFG spectra (ssp) of *d*-PS/cured BADGE buried interface before moisture exposure (closed circles) and after moisture exposure (open circles).

as well. This correlated to the loss of buried interfacial ordering of the epoxies seen after moisture exposure.

To summarize, buried interfaces between *d*-PS and the epoxies were probed with SFG. It was found that the uncured epoxies formed disordered interfaces with *d*-PS and therefore did not yield SFG signal. However, SFG spectra of the cured samples including both BADGE and BDDGE showed evidence of the epoxy methylene groups ordering at the buried interface. The formation of ordered buried interfaces was correlated to improved adhesion via lap shear tests. Additionally, moisture exposure was

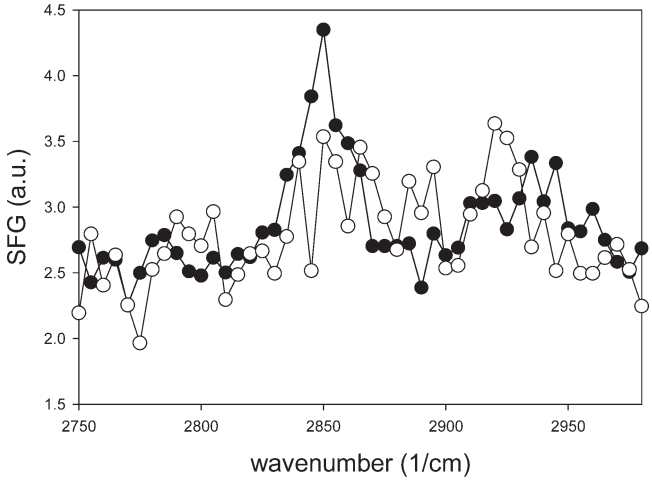

Figure 11. SFG spectra (ssp) of *d*-PS/cured BDDGE buried interface before moisture exposure (black circles) and after moisture exposure (open circles).

Table 10. Lap Shear Adhesion Testing Results from the *d*-PS/BADGE and *d*-PS/BDDGE Interfaces[a]

	BADGE/PS interfaces (MPa)	BDDGE/PS interfaces (MPa)
cured	4.47 ± 0.45	3.08 ± 0.57
cured after water exposure	3.45 ± 0.53	n/a

[a] Note n/a refers to an interface with negligible adhesion.

shown to decrease the order of the buried *d*-PS/cured epoxy interfaces, and this was correlated to decreased lap shear adhesion.

4. CONCLUSIONS

Developing an understanding of the adhesion of underfills in flip-chip devices is critical for designing improved underfill formulations to maximize flip-chip device performance. In these studies, SFG was used to study the surface structures of uncured

and cured epoxies used as underfills, as well as the buried interfaces between a model polymer and the underfill epoxies. It was found that an uncured bisphenol-type epoxy deposited differently on fused silica and polymeric substrates while an aliphatic-type epoxy did not. When epoxy-based underfills are deposited into flip-chip devices prior to cure, the underfill material comes into contact with a variety of substrates, and needs to be accounted for when designing underfill formulations.

Further, it was shown that the epoxy surface structures changed after they were cured. This has important implications for underfill design. Underfills are cured in situ in flip-chip devices. If specific surface structures are needed for the epoxy underfill to participate in specific adhesion mechanisms, any change in epoxy underfill surface structure during cure would affect adhesion, and needs to be understood. The effect of moisture exposure on epoxy surfaces was also investigated, and it was found that moisture caused surface reorientation of bisphenol-type epoxies but not aliphatic-type epoxies. Because moisture is known to cause delamination of epoxy underfills in flip-chip devices, it was important to determine how moisture exposure affected epoxy surface structure.

Lastly, the studies were expanded to buried interfaces between *d*-PS and the epoxies both before and after moisture exposure to better understand the structures at adhesive interfaces. It was shown that buried interfaces between *d*-PS and uncured epoxies were disordered. However, the buried interfaces between *d*-PS and cured epoxies did exhibit BADGE and BDDGE methylene ordering, and these interfaces adhered. Interfacial molecular ordering of the epoxy methylene backbones may be necessary for an adhesion mechanism to occur. Further, after moisture exposure, the interfacial epoxy ordering decreased, and adhesion strength diminished, most likely due to swelling-induced epoxy deformation.

This work explored surface and buried interfacial structures of epoxies used as underfills in flip-chip technology. It was shown that surface and buried interfacial structures could be correlated to adhesion strength, which could aid in the design of optimized underfills for flip-chip devices.

AUTHOR INFORMATION

Corresponding Author

*E-mail: zhanc@umich.edu. Fax: 734-647-4865.

Present Addresses

‡Department of Natural Sciences, Prairie State College, Chicago Heights, Ilinois 60411, United States

ACKNOWLEDGMENT

This work is supported by SRC (P10419). A.V.V. is supported by the Graduate Assistantships in Areas of National Need (GAANN).

REFERENCES

(1) Bae, J.-W.; Kim, W.; Park, S.-W.; Ha, C.-S.; Lee, J.-K. *J. Appl. Polym. Sci.* **2002**, *83*, 2617–2624.
(2) Ernst, L. J.; van't Hoff, C.; Yang, D. G.; Kiasat, M. S.; Zhang, G. Q.; Bressers, H. J. L.; den Boer, A. W. J.; Janssen, J. *J. Electron. Packag.* **2002**, *124*, 97–105.
(3) Ferguson, T. P.; Qu, J. *IEEE Trans.* **2006**, *29*, 105–111.
(4) Luo, S.; Wong, C. P. *IEEE Trans.* **2005**, *28*, 88–94.
(5) Lee, W. S.; Han, I. Y.; Yu, J.; Kim, S. J.; Byun, K. Y. *Thermochim. Acta* **2007**, *455*, 148–155.
(6) Yacobi, B. G.; Martin, S.; Davis, K.; Hudson, A.; Hubert, M. *J. Appl. Phys.* **2002**, *91*, 6227–6262.
(7) Arvanitopoulos, C. D.; Koenig, J. L. *Appl. Spectrosc.* **1996**, *50*, 11–18.
(8) Gonzalez-Benito. *J. Colloid Interface Sci.* **2003**, *267*, 326–332.
(9) Brahatheeswaran, C.; Gupta, V. B. *Polymer* **1993**, *34*, 289–294.
(10) Dufresne, A.; Lacabanne, C. *Polymer* **1995**, *36*, 4417–4424.
(11) Lange, J.; Toll, S.; Manson, J.-A. *Polymer* **1997**, *38*, 809–815.
(12) Ardebili, H.; Wong, E. H.; Pecht, M. *IEEE Trans.* **2003**, *26*, 206–214.
(13) Bain, C. D. *J. Chem. Soc., Faraday Trans.* **1995**, *91*, 1281–1296.
(14) Buck, M.; Himmelhaus, M. *J. Vac. Sci. Technol., A* **2001**, *19*, 2717–2736.
(15) Lambert, A. G.; Davies, P. B.; Neivandt, D. *J. Appl. Spectrosc. Rev.* **2005**, *40*, 103–145.
(16) Chen, Z. *Prog. Polym. Sci.* **2010**, *35*, 1376–1402.
(17) Shen, Y. R. *The Principles of Nonlinear Optics*; Wiley: New York, 1984.
(18) Chen, C.; Loch, C. L.; Wang, J.; Chen, Z. *J. Phys. Chem. B* **2002**, *107*, 10440–10445.
(19) Loch, C. L.; Ahn, D.; Chen, Z. *J. Phys. Chem. B* **2006**, *110*, 914–918.
(20) Loch, C. L.; Ahn, D.; Chen, C.; Wang, J.; Chen, Z. *Langmuir* **2004**, *20*, 5467–5473.
(21) Chen, C.; Wang, J.; Loch, C. L.; Ahn, D.; Chen, Z. *J. Am. Chem. Soc.* **2004**, *126*, 1174–1179.
(22) Loch, C. L.; Ahn, D.; Vázquez, A. V.; Chen, Z. *J. Colloid Interface Sci.* **2007**, *308*, 170–175.
(23) Wang, J.; Woodcock, S. E.; Buck, S. M.; Chen, C.; Chen, Z. *J. Am. Chem. Soc.* **2001**, *308*, 9470–9471.
(24) Wang, J.; Chen, C.; Buck, S. M.; Chen, Z. *J. Phys. Chem. B* **2001**, *105*, 12118–12125.
(25) Loch, C. L.; Ahn, D.; Chen, C.; Chen, Z. *J. Adhes.* **2005**, *81*, 319–345.
(26) Chen, C.; Wang, J.; Chen, Z. *Langmuir* **2004**, *20*, 10186–10193.
(27) Kristalyn, C. B.; Lu, X.; Weinman, , C. J.; Ober, C. K.; Kramer, E. J. *Langmuir* **2010**, *26*, 11337–11343.
(28) Chen, Z.; Shen, Y. R.; Somorjai, G. A. *Annu. Rev. Phys. Chem.* **2002**, *53*, 437–465.
(29) Gracias, D. H.; Chen, Z.; Shen, Y. R.; Somorjai, G. A. *Acc. Chem. Res.* **1999**, *32*, 930–940.
(30) Kweskin, S. J.; Komvopoulos, K.; Somorjai, G. A. *Langmuir* **2005**, *21*, 3647–3652.
(31) Ye, S.; Morita, S.; Li, G. F.; Noda, H.; Tanaka, M.; Uosaki, K.; Osawa, M. *Macromolecules* **2003**, *36*, 5694–5703.
(32) Yurdumakan, B.; Nanjndiah, K.; Dhinojwala, A. *J. Phys. Chem. C* **2007**, *111*, 960–965.
(33) Ye, H. K.; Gu, Z. Y.; Gracias, D. H. *Langmuir.* **2006**, *22*, 1863–1868.
(34) Opdahl, A.; Phillips, R. A.; Somorjai, G. A. *J. Polym. Sci., Part B* **2004**, *42*, 421–432.
(35) Li, Q. F.; Hua, R.; Chea, I. J.; Chou, K. C. *J. Phys. Chem. B* **2008**, *112*, 694–697.
(36) Briggman, K. A.; Stephenson, J. C.; Wallace, W. E.; Richter, L. J. *J. Phys. Chem. B* **2001**, *105*, 2785–2791.
(37) Chen, Z. *Polym. Int.* **2006**, *56*, 577–587.
(38) Ye, S.; McClelland, A.; Majumdar, P.; Stafslien, S.; Daniels, J.; Chisholm, B.; Chen, Z. *Langmuir* **2008**, *24*, 9686–9694.
(39) Vázquez, A. V.; Shephard, N. E.; Steinecker, C. L.; Ahn, D.; Spanninga, S.; Chen, Z. *J. Colloid Interface Sci.* **2009**, *331*, 408–416.
(40) Vázquez, A. V.; Boughton, A. P.; Shephard, N. E.; Rhodes, S. M.; Chen, Z. *ACS Appl. Mater. Interf.* **2010**, *2*, 96–103.
(41) Yurdumakan, B.; Harp, G. P.; Tsige, M.; Dhinojwala, A. *Langmuir* **2005**, *21*, 10316–10319.
(42) Kataoka, S.; Cremer, P. S. *J. Am. Chem. Soc.* **2006**, *128*, 5516–5522.
(43) Hirose, C.; Akamatsu, N.; Damen, K. *Appl. Spectrosc.* **1992**, *46*, 1051–1072.

(44) Duffy, D.; Davies, P.; Bain, C. *J. Phys. Chem.* **1995**, *99*, 15241–15246.
(45) Lu, R.; Gan, W.; Wu, B. H.; Chen, H.; Wang, H. F. *J. Phys. Chem. B* **2004**, *108*, 7297–7306.
(46) Chen, C.; Wang, J.; Woodcock, S.; Chen, Z. *Langmuir.* **2002**, *18*, 1302–1309.
(47) Lu, X.; Han, J.; Shephard, N.; Rhodes, S.; Martin, A.; Li, D.; Xue, G.; Chen, Z. *J. Phys. Chem. B* **2009**, *113*, 12944–12951.
(48) Chen, C. Y.; Wang, J.; Even, M. A.; Chen, Z. *Macromolecules* **2002**, *35*, 8093–8097.
(49) Hirose, C.; Akamatsu, N.; Domen, K. *J. Chem. Phys.* **1992**, *96*, 997–1004.
(50) Hirose, C.; Yamamoto, H.; Akamatsu, N.; Domen, K. *J. Phys. Chem.* **1993**, *97*, 10064–10069.
(51) Lu, X.; Spanninga, S. A.; Kristalyn, C. B.; Chen, Z. *Langmuir* **2010**, *26*, 14231–14235.
(52) Snyder, R. G.; Strauss, H. L.; Elliger, C. A. *J. Phys. Chem.* **1982**, *86*, 5145–5150.
(53) Macphail, R. A.; Strauss, H. L.; Snyder, R. G.; Elliger, C. A. *J. Phys. Chem.* **1984**, *88*, 334–341.
(54) Carrasco, F.; Pages, P.; Lacorte, T.; Briceno, K. *J. Appl. Polym. Sci.* **2005**, *98*, 1524–1535.